Explicit Solutions of the Bethe Ansatz Equations for Bloch Electrons in a Magnetic Field

Yasuhiro Hatsugai,[1,*] Mahito Kohmoto,[1] and Yong-Shi Wu[2]

[1]*Institute for Solid State Phyiscs, University of Tokyo, 7-22-1 Roppongi Minato-ku, Tokyo 106, Japan*
[2]*Department of Physics, University of Utah, Salt Lake City, Utah 84112*
(Received 26 April 1994)

For Bloch electrons in a magnetic field, explicit solutions are obtained at the center of the spectrum for the Bethe ansatz equations of Wiegmann and Zabrodin. When the magnetic flux per plaquette is $1/Q$ with Q an odd integer, distribution of the roots of the Bethe ansatz equation is uniform except at two points on the unit circle in the complex plane. For the semiclassical limit $Q \to \infty$, the wave function is $|\psi(x)|^2 = (2/\sin \pi x)$, which is critical and unnormalizable. For the golden-mean flux, the distribution of roots has exact self-similarity and the distribution function is nowhere differentiable. The corresponding wave function also shows a clear self-similar structure.

The Azbel-Hofstadter-Wannier problem of two-dimensional Bloch electrons in a magnetic field is an old problem that often brings new excitement. The equations of motion can be reduced to one-dimensional ones, which appear in many different physical contexts, ranging from the quantum Hall effect [1] to quasiperiodic systems (for a review, see, for example, Ref. [2]). Its topological character has been revealed both for periodic boundary conditions [1] and for systems with edges [3]. The interplay of two intrinsic periods, the period of the lattice and that of the magnetic flux, is essential in this problem. Previously many studies were done for the cases when the two periods are commensurable, i.e., the magnetic flux per plaquette ϕ is rational. But the incommensurate cases (with an irrational ϕ) are more interesting in that the spectrum is known to have an extremely rich structure like the Cantor set and to exhibit multifractal behavior [2,4]. Another interesting case is the weak field limit: When the flux is small, the semiclassical treatment of the WKB type is justified. Although some properties of the wave functions are known [5,6], much of the knowledge we have came from numerical studies for rational fluxes [2]. In this Letter, we derive several analytical results for the weak-field limit and for the incommensurate golden-mean flux, by following the highly innovative Bethe ansatz approach recently proposed by Wiegmann and Zabrodin [7] using quantum group techniques.

The Hamiltonian is given by $H = \sum_{m,n}(c^\dagger_{m+1,n}e^{i\theta^x_{m,n}} \times c_{m,n} + c^\dagger_{m,n+1}e^{i\theta^y_{m,n}}c_{m,n} + \text{H.c.})$ where $c_{m,n}$ is the annihilation operator for an electron at site (m,n). We first assume the flux per plaquette ϕ is rational: $\phi = P/Q$ with coprime odd integers P and Q, and later take appropriate limits of ϕ. Let us take the diagonal gauge, $\theta^x_{m,n} = +\pi\phi(n + m)$, $\theta^y_{m,n} = -\pi\phi(n + m)$ [9]. Then the Schrödinger equation for the one particle state $|\Psi\rangle = \sum_{m,n} \psi_{m,n}c^\dagger_{m,n}|0\rangle$ is written as $i(q^{l+1} + q^{-l})\Psi_{l+1} - i(q^{l-1} + q^{-l})\Psi_{l-1} = E\Psi_l$ at the midband point where $\psi_{m,n} = i^{m+n}\Psi_{m+n}$ and $q = e^{i\pi\phi} = e^{i\pi P/Q}$. Wiegmann and Zabrodin observed [7] that if we write $\Psi_l = \Psi(q^l)$

with $\Psi(z)$ a polynomial of degree $Q - 1$, this difference equation coincides with the eigenequation of a combination of generators of the quantum group $U_q(sl_2)$ in the representation provided by $\Psi(z)$. Thus the zeros, $\{z_l\}$, of the polynomial $\Psi(z)$ must satisfy the Bethe ansatz equations (BAE) [7]

$$\frac{z_l^2 + q}{qz_l^2 + 1} = -\prod_{m=1}^{Q-1}\frac{qz_l - z_m}{z_l - qz_m}, \quad l = 1,\ldots,Q - 1. \quad (1)$$

For the zero energy $E = 0$, they showed that $\Psi(z)$ is given by the so-called continuous q ultraspherical polynomial [10] as $\Psi(z) = \frac{(q^2;q^2)_n}{(q;q^2)_n}(-iz)^n P_n(-iz)$, where $P_n(z) = \sum_{k=0}^{n}\frac{(q;q^2)_k(q;q^2)_{n-k}}{(q^2;q^2)_k(q^2;q^2)_{n-k}}z^{n-2k}$, $n = (Q - 1)/2$, and $(a;q)_k = \prod_{m=0}^{k-1}(1 - aq^m)$ [11].

In order to understand the properties of the wave functions at $E = 0$, the center of the spectrum, we try to solve the BAE (1) explicitly. It can be shown from the above definition of the polynomial $P_n(z)$ that it satisfies a difference equation

$$(1 - qz^2)P_n(qz) + (q - z^2)P_n(q^{-1}z) = 0. \quad (2)$$

Put $z = q^{\pm 1/2}$, then we get $P_n(q^{\pm 3/2}) = 0$. So $q^{\pm 3/2}$ are roots. By iteration, the complete set of roots of the BAE are given by

$$z_m = iq^{2m-1/2}, iq^{-2m+1/2}, \quad m = 1,\ldots,(Q - 1)/2. \quad (3)$$

They are all on the unit circle. Let us write the roots as $z_m = e^{i\theta_m}$ and consider the distribution of θ_m.

Consider first the special case $P = 1$. The roots $\{z_m\}$ distribute uniformly on the unit circle except near $z = \pm i$. The roots for $Q = 21$ are shown in Fig. 1. In the semiclassical limit $Q \to \infty$, that is, $q \to 1$, the distribution function $\rho(\theta) = \lim_{Q\to\infty} Q\Delta\theta$ is smooth (constant) where $\Delta\theta = \theta_{m+1} - \theta_m$. Continuous behavior of $\rho(\theta)$ is usually obtained in the exactly solvable models (the Heisenberg chain, the Hubbard chain, etc.) in which $\rho(\theta)$ is determined by an integral equation.
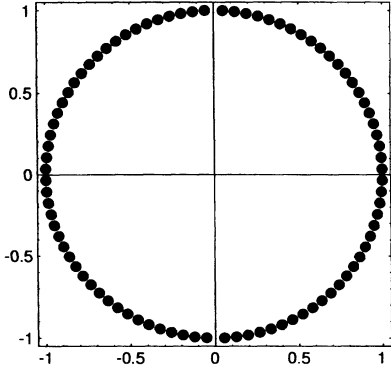
FIG. 1. Roots of the Bethe ansatz equation for the special case $P = 1$ and $Q = 89$.

FIG. 2. Roots of the Bethe ansatz equation for the ratio of the Fibonacci numbers. $\phi_k = P_k/Q_k = 3/5$, $13/21$, $55/89$, $233/377$, $987/1597$, and $4181/6765$ (a) in the whole complex plane. (b) An enlarged figure. In each case, the roots are always on the unit circle. We scaled the radii to show the branching rule clearly.

When the flux is irrational, the situation is quite different. Take the flux $\phi = 1/\tau = (\sqrt{5} - 1)/2$, where τ is the golden mean. To reach this flux, we consider a sequence of rational fluxes $\phi_k = P_k/Q_k$, where $Q_k = F_{3k+1}, P_k = F_{3k}$, and F_k is a Fibonacci number defined by $F_{k+1} = F_k + F_{k-1}, F_1 = 1, F_0 = 1$. In this case, the two types of roots in Eq. (3) are nested. To gain an insight into the distribution of roots, it is helpful to consider the pseudo roots which are defined also by Eq. (3) but with the range of m modified to $m = -(Q - 1)/2, \cdots, 0$. In Fig. 2 we show the distributions of the roots (black points) and pseudo roots (gray points) for several $\phi_k (k = 1, 2, 3, 4, 5, 6)$. Here the radius of the unit circle has been scaled so as to show all the cases at once. These figures clearly show that there is a branching rule for the true roots (denoted by A) and pseudo roots (by B) as follows:

$$A^3 \rightarrow A^3 B^2 A^3 B^2 A^3 ,$$

$$A^2 \rightarrow A^3 B^2 A^3 ,$$

$$B^3 \rightarrow B^3 A^2 B^3 A^2 B^3 ,$$

$$B^2 \rightarrow B^3 A^2 B^3 . \qquad (4)$$

The initial condition is $B^3 A^2 B^3 A^2$ (cyclic). In the kth stage of the sequence, the number of clusters of the true roots A^3 and A^2 are $Q_{k-1} - 1$ and $P_{k-1} + 1$, respectively. This branching rule gives rise to a self-similar structure for the distribution $\rho(\theta)$ in the limit $k \rightarrow \infty$. To characterize the distribution, let us define the generation of a root. According to the branching rule (4), each true (pseudo) root branches into a cluster of 3 new true (pseudo) roots, each of which in a sense has a parent. At the same time, between these clusters of new pseudo (true) roots, there is a pair of new-born true (pseudo) roots which have no parent. We assign the generation number to a root so that it is 1 when the root does not have a parent; otherwise it is 1 plus that of its parent. Let us denote the number of true (pseudo) roots in the kth stage with generation g by $n_A(g, k)[n_B(g, k)](g = 1, \ldots, k)$. [Then in the special case $P = 1$, $n_A(g, k) = n_B(g, k) = \delta_{kg}$.] In the present
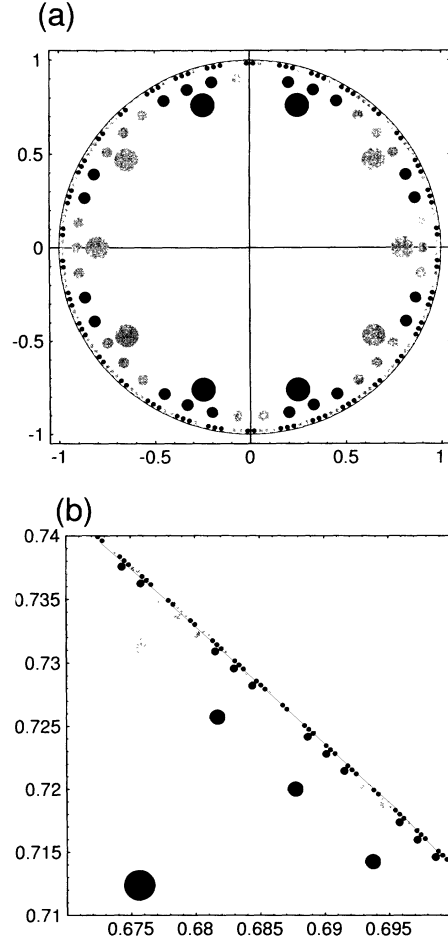
case, we get a recursion formula by the branching rule as $n_A(g, k) = 3 n_A(g - 1, k - 1)$, $g = 2, \ldots, k$, $n_A(1, k) = 2(P_{k-1} + 1)$. Thus $n_A(g, k) = 2 \times 3^{g-1}(P_{k-g} + 1)$ and $n_B(g, k) = 2 \times 3^{g-1}(P_{k-g} - 1)$. The above considerations exemplify the difference of the distributions between the semiclassical limit and the incommensurate case. The distribution of the roots has a self-similar structure and the function $\rho(\theta)$ is nowhere differentiable in the incommensurate limit, while that for the semiclassical limit is smooth. We believe this is characteristic to the incommensurate case.

Another way to characterize the distribution is to map to the dual (reciprocal) space. This can be done for arbitrary P and Q. We lift the θ_m to the real axis periodically. On the real axis, the true and pseudo roots occupy a lattice of points $\{j/2Q | j: \text{integer}\}$ with spacing $1/2Q$. Thus we perform the Fourier transform by $S_Q(p) = \sum_{j=-\infty}^{\infty} e^{ipj} \tilde{S}_Q(j)$ where $\tilde{S}_Q(j)$ is the so-called

defining function: $\tilde{S}_Q(j) = 1$ if there is a true root at $j/2Q$, otherwise $\tilde{S}_Q(j) = 0$. Then

$$S_Q(p) = \frac{\pi}{Q} \sum_{r=0}^{Q-1} s_Q^r \, \delta(p - p_r), \qquad 0 \le p < 2\pi, \quad (5)$$

where $s_Q^0 = (Q - 1)$, $s_Q^r = (-)^{r+1}[\cos(\frac{1}{2}Pp_r)]^{-1}$ $(r = 1, \dots, Q - 1)$, and $p_r = 2\pi r/Q$. In the semiclassical limit, $|S_Q(p)|^2$ is well defined and behaves smoothly. On the other hand, $|S_Q(p)|^2$ is not even differentiable in the incommensurate limit since $P \rightarrow \infty$. Also it can be shown that the original defining function is given by

$$\tilde{S}_Q(j) = \left(\frac{1}{2Q}\right) \sum_{n=1}^{Q-1} [1 - (-)^n$$

$$\times \cos\left(2\pi jn/Q\right) / \cos\left(\pi Pn/Q\right)].$$

Next let us consider the wave function. Using the explicit roots we found above, the wave function at site j can be written in a compact factorized form

$$\Psi_j = (-q)^{-j}(iq^{-j+3/2}; q^2)_{(Q-1)/2}(iq^{-j-3/2}; q^{-2})_{(Q-1)/2}. \tag{6}$$

It is convenient to shift the site, $\bar{j} = j + j_0$, by an amount j_0 where j_0 is determined by $Pj_0 = (Q - P)/2 \pmod{2Q}$. Then $\Psi_{\bar{j}} = 0$ at $\bar{j} = 2m, -2m + 1$ $[m = 1, \dots, (Q - 1)/2]$, and the wave function is nonzero only at $\bar{j} = 1, 3, \dots, 2Q$ and $Q + 1, Q + 3, \dots, 2Q$. Using Eq. (6), the amplitude of the wave function is calculated as

$$|\Psi_{\bar{j}}|^2 = \prod_{m=1}^{(Q-1)/2} \left| 4 \sin \frac{\pi(2m - \bar{j})P}{2Q} \right.$$

$$\left. \times \sin \frac{\pi(2m + \bar{j} - 1)P}{2Q} \right|^2. \tag{7}$$

First let us present the exact results explicitly for the special case $P = 1$. A direct and careful calculation leads to a very simple result for the amplitude

$$|\psi(x)|^2 = \frac{2}{\sin(\pi x)}, \qquad (0 < x < 1), \tag{8}$$

up to a constant factor, where $\psi(x) = \Psi_{\bar{j}}$, $x = (2\bar{j} - 1)/2Q$, and the semiclassical limit $Q \rightarrow \infty$ is taken. Thus the squared amplitude of the wave function is given by the inverse chord distance in the semiclassical limit. The recursion relation $|\Psi_{\bar{j}}|^2 = |\Psi_{\bar{j}-2}|^2 \sin^2[\pi(\bar{j} - 2)/Q]/\sin^2[\pi(\bar{j} - 1)/Q]$ obtained from Eq. (7), has played a key role [12]. For a finite Q, a correction factor appears only near the edges ($x = 0$ and 1). For example, near the edge $x \approx 0$, the finite size correction is given by $|\psi(x_{2l+1})|^2 = C(l)(2/\sin \pi x_{2l+1})$, with $C(l) = \pi(l + 1/4)\prod_{k=1}^{l}(1 - 1/2k)^2$, where $C(0) = \pi/4 = 0.78539\dots, C(1) = 5\pi/16 = 0.98174\dots, C(2) =$

$81\pi/256 = 0.99402\dots, \dots, \dots$. So the finite-size correction factor $C(l)$ converges to unity very rapidly and Eq. (7) is quite accurate even at small Q. The norm of the wave function is $\log Q + $ const and unnormalizable, which is characteristic of a critical wave function. In Fig. 3, the amplitudes of the analytic wave functions, normalized by the peak height, are shown for several values of Q.

Next let us discuss the case with golden-mean flux. We plot the analytic results Eq. (7) in Fig. 4 for a sequence of rational fluxes converging to $1/\tau$. One can easily recognize the self-similar behavior of the wave function. Each peak branches into three peaks in the next stage. Presumably these are the reflection of the self-similar distribution of the roots, Eq. (4). The multifractal analysis [2] done numerically gives a smooth $f(\alpha)$ shown in Fig. 5. This clearly shows that this wave function is multifractal and critical. We note the striking resemblance of these wave functions to that of the 1D quasicrystal Fibonacci lattice at the center of the spectrum [13]. An analytical derivation of $f(\alpha)$ is under progress. The latter was obtained exactly by a different technique and $f(\alpha)$ is obtained analytically [14].

In conclusion, we have found analytical solutions to the BAE (1) that describe the Bloch state in a magnetic field with zero energy. The flux per plaquette is $\phi = P/Q$ with coprime odd integers P and Q. All roots are on the unit circle, and the defining function for the roots is explicitly derived.

When $P = 1$, the roots distribute uniformly for any odd Q. In the semiclassical limit $Q \rightarrow \infty$, the density function of roots is smooth. When the flux ϕ are ratios of the successive Fibonacci numbers which converge to the golden mean, we found the branching rule for the roots, which makes the density function ρ of the roots exactly self-similar and nowhere differentiable.

We are able to get explicit wave functions too. In the semiclassical case, a compact expression is derived
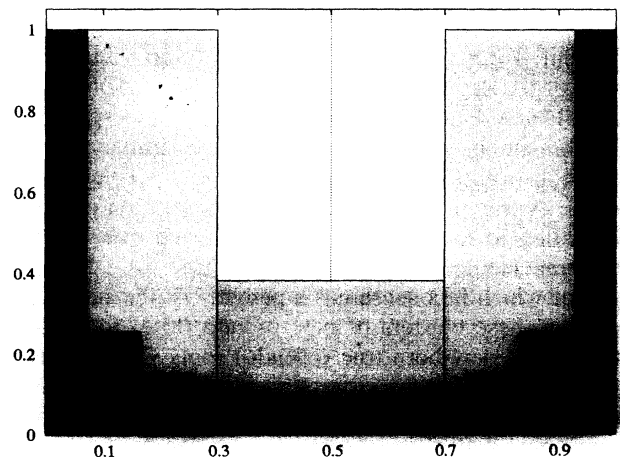

FIG. 3. Squared amplitudes for the wave functions: the special cases $P = 1$ and $Q = 5, 21, 89, 377$. The wave functions are normalized by the peak heights.
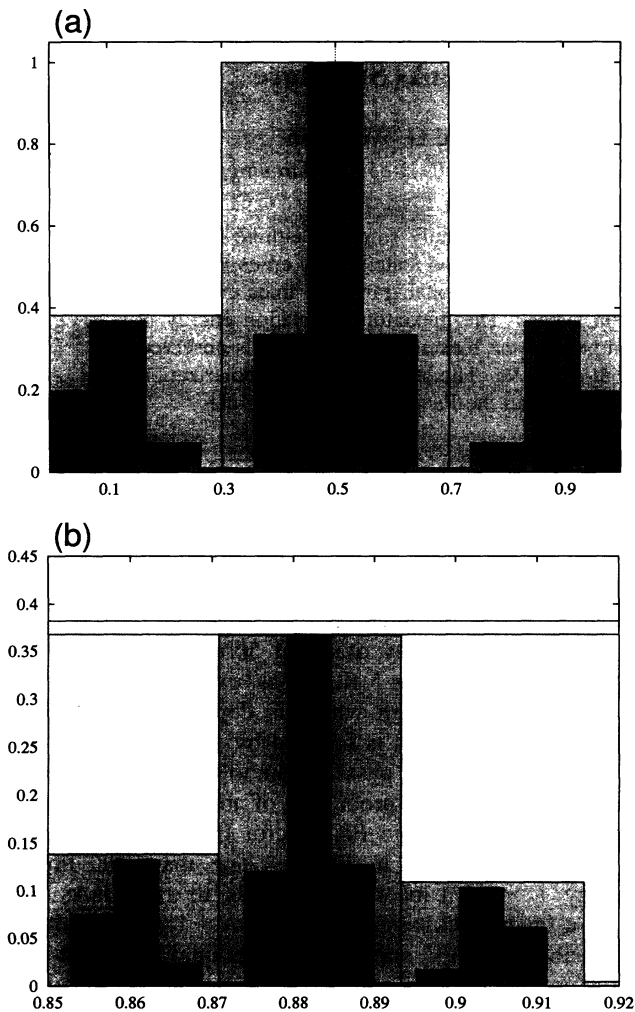
FIG. 4. Amplitude of the wave functions: for the ratios of successive Fibonacci numbers: (a) whole region ($\phi = 3/5$, 13/21, and 55/89) and (b) enlarged plot of the region near 0.89 ($\phi = P_k/Q_k = 3/5$, 13/21, 55/89, 233/377, 987/1597, and 4181/6765). The wave function with a larger value of Q is shaded darker. The wave functions are normalized by the peak height.

for the critical wave function, which turns out to be not normalizable. The squared amplitude, $|\psi(x)|^2$, is given by the inverse chord distance, $2/\sin(\pi x)$. For the golden-mean flux, the wave function also has a clear self-similar branching structure.

Finally we remark that the solutions (3) to the BAE have a relatively simple structure, and positions of the roots are not affected by a finite Q correction. These facts together with the simple form (8) of the amplitude of the wave functions suggest that the symmetry of the problem, at least at the center of the spectrum, is higher than originally expected. It might just be the quantum group $U_q(sl_2)$, though a clear-cut proof is still lacking. The situation would be similar to the Haldane-Shastry
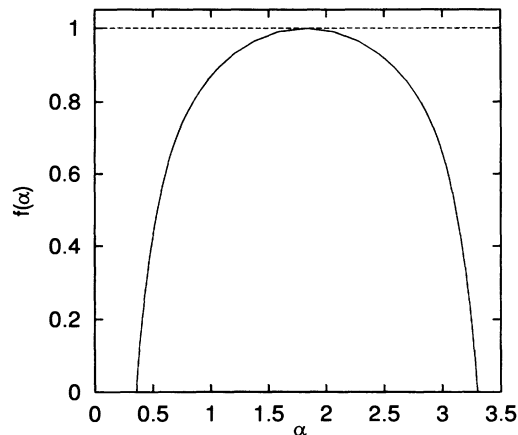

FIG. 5. The plot of $f(\alpha)$ for the wave function in the golden-mean case.

model where the symmetry is known to be higher than what is naively expected [15,16].

*Electronic mail address: hatsugai@tansei.cc.u-tokyo.ac.jp

[1] D. J. Thouless, M. Kohmoto, P. Nightingale, and M. den Nijs, Phys. Rev. Lett. 49, 405 (1982).

[2] H. Hiramoto and M. Kohmoto, Int. J. Mod. Phys. B 6, 281 (1992).

[3] Y. Hatsugai, Phys. Rev. B 48, 11 851 (1993); Phys. Rev. Lett. 71, 3697 (1993).

[4] D. R. Hofstadter, Phys. Rev. B 14, 2239 (1976).

[5] D. J. Thouless and Q. Niu, J. Phys. A 16, 1911 (1983).

[6] S. Aubry and G. André, Ann. Israel Phys. Soc. 3, 131 (1980).

[7] P. B. Wiegmann and A. V. Zabrodin, Phys. Rev. Lett. 72, 1890 (1994). See also Ref. [8].

[8] L. D. Fadeev and R. M. Kashaev, University of Helsinki Report No. HU-TFT-93-63 (to be published).

[9] M. Kohmoto and Y. Hatsugai, Phys. Rev. B 41, 9527 (1990).

[10] This $P_n(z)$ is obtained from the continuous q ultraspherical polynomials as $P_n(z) = C_n([(z + z^{-1})/2]; q|q^2)$. See G. Gasper and M. Rahman, Basic Hypergeometric Series (Cambridge Univ. Press, New York, 1990), p. 169.

[11] Our 1D difference equation (in the diagonal gauge) at $E = 0$ has another solution which is given by $\tilde{\Psi}_l = \tilde{\Psi}(q^l)$ where $\tilde{\Psi}(z) = \frac{(q^2;q^2)_n}{(q;q^2)_n} (-iz^{-1})^{n+1} P_n(iz^{-1})$, which has a pole at $z = 0$. This solution does not satisfy the pole free condition, and a separate consideration is needed. However, since $\{z_m\} = \{z_m^*\}$ as shown later, we have $|\Psi_l| = |\tilde{\Psi}_l|$. Thus we only consider Ψ_l from now on.

[12] $|\Psi_{j=1}|^2 = Q$ for arbitrary $\phi = P/Q$.

[13] M. Kohmoto and J. R. Banavar, Phys. Rev. B 34, 563 (1986).

[14] T. Fujiwara, M. Kohmoto, and T. Tokihiro, Phys. Rev. B 40, 7413 (1989).

[15] F. D. M. Haldane, Phys. Rev. Lett. 60, 635 (1988); F. D. M. Haldane, Z. N. C. Ha, J. C. Talstra, D. Bernard, and V. Pasquier, Phys. Rev. Lett. 69, 2021 (1992),

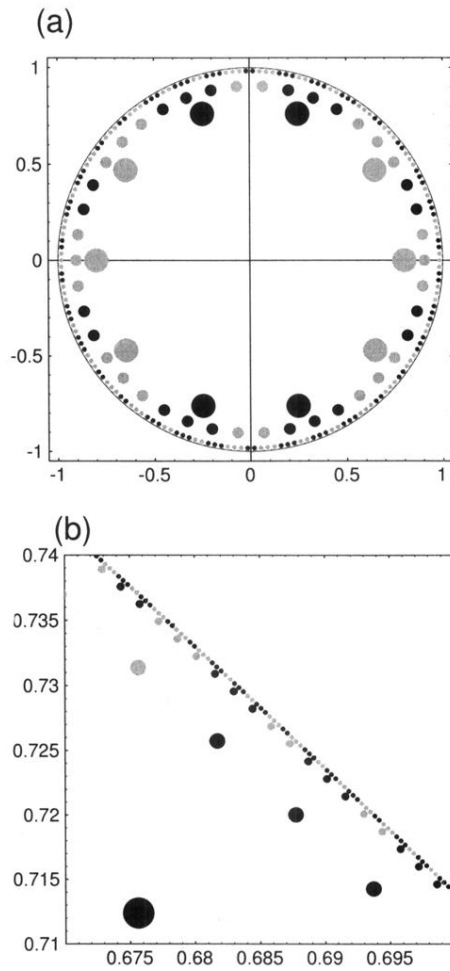[16] B. S. Shastry, Phys. Rev. Lett. 60, 639 (1988).

FIG. 2. Roots of the Bethe ansatz equation for the ratio of the Fibonacci numbers. $\phi_k = P_k/Q_k = 3/5$, $13/21$, $55/89$, $233/377$, $987/1597$, and $4181/6765$ (a) in the whole complex plane. (b) An enlarged figure. In each case, the roots are always on the unit circle. We scaled the radii to show the branching rule clearly.
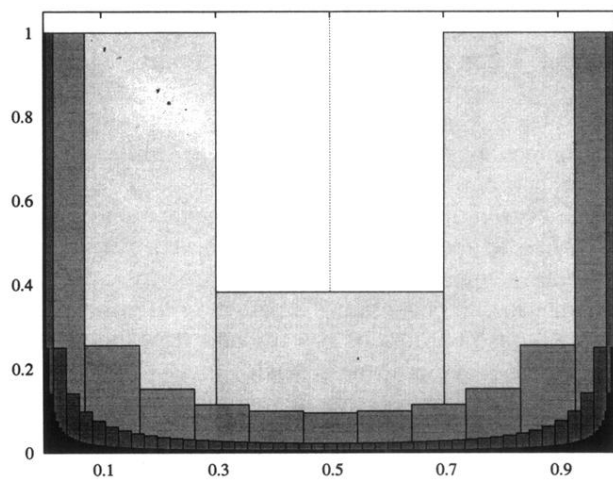
FIG. 3. Squared amplitudes for the wave functions: the special cases $P = 1$ and $Q = 5, 21, 89, 377$. The wave functions are normalized by the peak heights.
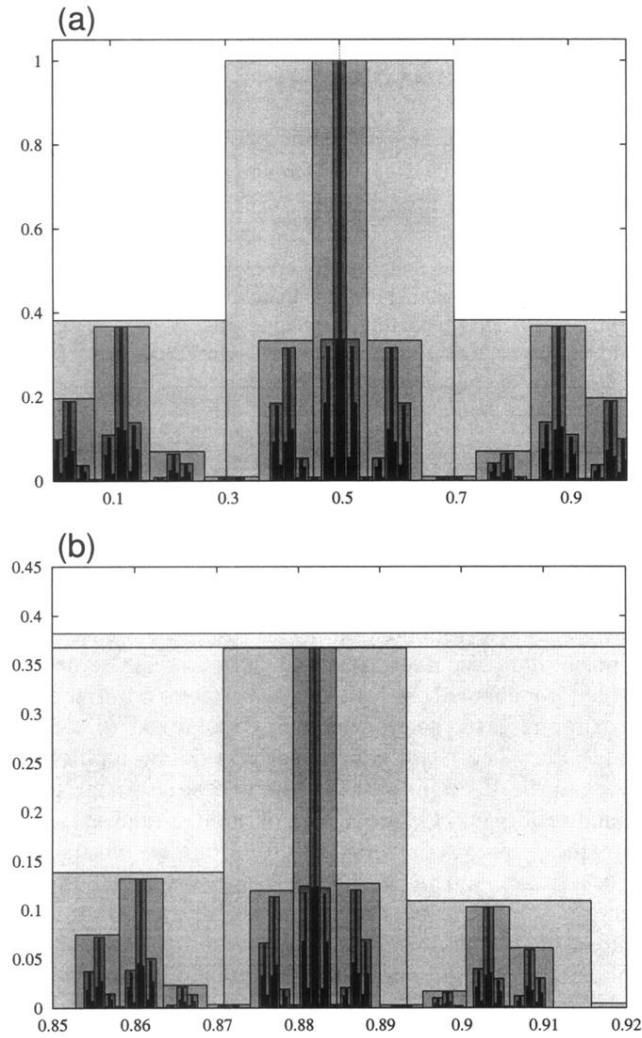
FIG. 4. Amplitude of the wave functions: for the ratios of successive Fibonacci numbers: (a) whole region ($\phi = 3/5$, $13/21$, and $55/89$) and (b) enlarged plot of the region near 0.89 ($\phi = P_k/Q_k = 3/5$, $13/21$, $55/89$, $233/377$, $987/1597$, and $4181/6765$). The wave function with a larger value of Q is shaded darker. The wave functions are normalized by the peak height.